

# Quantum Jump Metrology with Quantum Feedback in Cavity Networks

Kawthar Al Rasbi,<sup>1,2</sup> Almut Beige<sup>1</sup> and Lewis A. Clark<sup>3</sup>

<sup>1</sup>*The School of Physics and Astronomy, University of Leeds, Leeds LS2 9JT, United Kingdom*

<sup>2</sup>*The Department of Physics, Sultan Qaboos University, Sultanate of Oman and*

<sup>3</sup>*Centre for Quantum Optical Technologies, Centre of New Technologies,  
University of Warsaw, Banacha 2c, 02-097 Warsaw, Poland*

(Dated: January 13, 2022)

Quantum metrology enhances measurement precision by utilising the properties of quantum physics. In interferometry, this is typically achieved by evolving highly-entangled quantum states before performing single-shot measurements to reveal information about an unknown phase. While this is the theoretical optimum approach, implementation with all but the smallest states is still extremely challenging. An alternative approach is quantum jump metrology, which deduces information by continuously monitoring an open quantum system while inducing phase-dependent temporal correlations with the help of quantum feedback. Taking this approach here, we analyse measurements of a relative phase in an optical network of two cavities with quantum feedback in the form of laser pulses. It is shown that the proposed scheme can exceed the standard quantum limit without the need for complex quantum states.

PACS numbers:

## I. INTRODUCTION

Highly accurate measurements are important for a variety of applications, ranging from probing biological samples [1–3] to the detection of gravitational waves [4]. Often, such measurements use light passing through interferometric devices. Classically, it is well understood how to execute such measurements effectively [5–10]. One way of increasing their precision is to use higher intensity sources. Sometimes this is not possible, for example, if the object to be probed is fragile or has a short lifetime [2]. In such cases, precise estimations can only be made after repeating measurements many times. More recently however, it was recognised that alternatively one could explore the properties of quantum physics, specifically through quantum metrology [11–13]. These can allow for an increased precision of measurements given the same number of probes.

Suppose an unknown parameter  $\varphi$  is determined by performing exactly  $N$  independent measurements, as illustrated in Fig. 1(a). In this case, the scaling of the uncertainty  $\Delta\hat{\varphi}$  of the estimator with the number of probes  $N$  is limited by the standard quantum limit, which tells us that

$$(\Delta\hat{\varphi})^2 \propto \frac{1}{N}. \quad (1)$$

However, for correlated probes, this scaling can be improved. For maximally correlated probes, the Heisenberg limit may be obtained, which scales with the number of probes as

$$(\Delta\hat{\varphi})^2 \propto \frac{1}{N^2}. \quad (2)$$

This means that for large  $N$ , the parameter  $\varphi$  can be estimated with the same precision with fewer probes. Determining how to obtain and utilise such correlated probes has thus been an active area of research.

As illustrated in Fig. 1(b), one solution is to evolve entangled quantum states in a  $\varphi$ -dependent fashion followed by a collective measurement of their state [14–22]. However, a typical problem with this approach is that it is difficult to implement. For example, it has been shown that so-called N00N states, which are highly-entangled  $N$  photon states, are optimal for quantum interferometry experiments [18–20, 23–26]. But obtaining a reasonably large  $N$  in the laboratory to realise the above-described enhancement remains extremely challenging [27, 28]. Fortunately, using entanglement is not the only way of enhancing measurement precision [29–34]. For example, in Ref. [30], it has been shown that another way of overcoming the standard quantum limit in Eq. (1) is by using non-linear or interacting systems. Taking this approach, the uncertainty  $\Delta\hat{\varphi}$  can scale such that

$$(\Delta\hat{\varphi})^2 \propto \frac{1}{N^k}, \quad (3)$$

where  $k$  is the order of the non-linearity of the interaction. Once again though, non-linearities are often hard to implement experimentally, particularly when processing information with light.

In this paper we adopt an alternative approach and use *quantum jump metrology* [35, 36] to improve the precision of measurements. Quantum jump metrology does not require the preparation of highly entangled quantum states nor the presence of non-linear optical elements and is therefore relatively easy to implement. Its basic idea is to deduce information about an unknown parameter  $\varphi$  by monitoring the output statistics of an open quantum system. To ensure that the dynamics of the individual quantum trajectories of the system depend on  $\varphi$ , we use quantum feedback [37] which is triggered by certain measurements outcomes, as illustrated in Fig. 1(c). Using the dynamics of open quantum systems to infer information about an unknown parameter recently received a lot of attention in the literature [38–41].

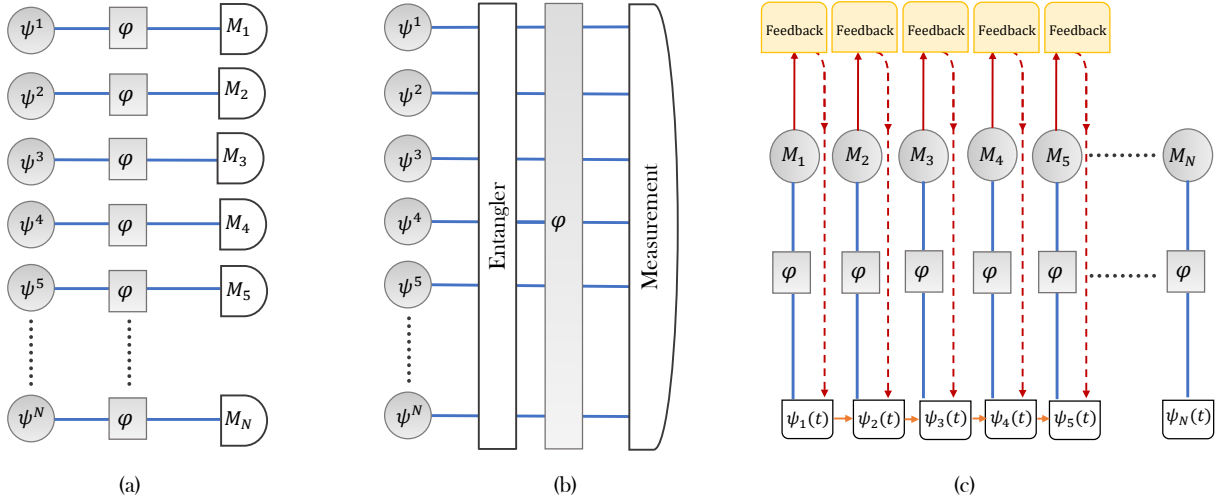


FIG. 1: A comparison of three general schemes to achieve an enhancement in estimating an unknown parameter  $\varphi$ . (a) Classical scheme consisting of independent and uncorrelated systems where each probe is encoded with the parameter to be determined and then measured. In such a case the accuracy of measurement is limited by the Standard Quantum Limit. (b) Quantum mechanical scheme utilising entangled states give rise to higher measurement accuracy reaching the Heisenberg Limit. (c) Quantum jump metrology scheme where the quantum system is evolved in time inside an instantaneous feedback loop. Sequential measurements on the system allows for accuracy enhancement beyond the standard quantum limit due to the existence of temporal correlations.

Ref. [35] introduced a quantum metrology scheme for measuring the phase difference between a coherent state prepared inside an optical cavity and a laser providing feedback pulses. In this paper, we propose instead a scheme which simply measures the difference  $\tilde{\varphi}$  between two phases  $\varphi_1$  and  $\varphi_2$  corresponding to two pathways through a linear optics setup, which is shown in Fig. 2. The setup that we consider here is easier to implement and much more practical than the original protocol [35]. Nevertheless, the scheme that we propose here too relies only on coherent states, yet it is capable of producing correlated photon statistics and thus surpassing the standard scaling due to the presence of quantum feedback. Hence, as well as demonstrating a simple scheme with enhanced sensing capabilities, our proposal also demonstrates the power of using quantum feedback to obtain quantum effects, even in ‘classical-like’ states such as coherent states.

The use of quantum feedback has found a variety of applications not only in quantum metrology [35, 36], but also in quantum error correction and noise reduction [42], quantum state stabilisation [43], entanglement control [44] and in implementing Hidden Quantum Markov Models [45]. Moreover, it has recently been shown that quantum feedback can lead to ergodicity breaking in quantum optical systems [46]. This can again be achieved even with coherent states and feedback in the form of displacements of the field, thus only requiring relatively simple technology to implement. Intuitively, it is easy to see how quantum feedback can lead to correlations in the bath statistics of an open quantum system. Consider

a quantum optical system that emits a photon at time  $t_1$ . Then as the system is perturbed by the feedback the emission probability for another photon is altered. Thus, the emission at time  $t_2$  is correlated with the emission at  $t_1$ . If this feedback depends on an unknown parameter, these correlations can be used to gain information for its estimation. Hence it is not surprising that quantum feedback is a powerful tool for quantum technology tasks.

Although Fig. 2 shows two optical cavities, the quantum metrology which we propose here could also be implemented using only a single cavity. In this case, the two different polarisations of light and of the states inside an optical cavity need to be utilised. Moreover, lasers 1 and 2 would have to differ in polarisation and each beam splitter would have to be replaced by a single polarising beam splitter. However, for simplicity, we analyse in the following the experimental setup shown in Fig. 2. In recent years, much progress has been made in implementing optical cavities which confine photons for a relatively long time. For example, strong fibre-integrated cavities [47] have already become available in laboratories worldwide. Moreover, much progress has been made in miniaturising and increasing the efficiency of single photon detectors [48]. The proposed quantum metrology scheme is hence feasible with current technology.

This paper is structured as follows. In Section II, we introduce the notation and the basic theoretical models for the modelling of the linear optics cavity network shown in Fig. 2. Afterwards, in Section III, we introduce the measurement scheme that we propose in this paper to

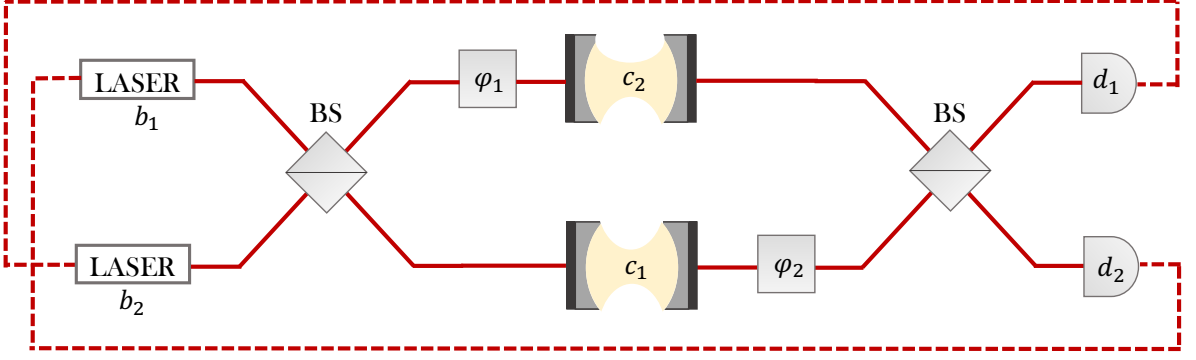


FIG. 2: Two optical cavities are monitored through a linear optics network with photon detectors. Upon the detection of a photon, quantum feedback is triggered and applied to the cavities, also through a linear optics network. In this diagram and our subsequent analysis of the system, we consider a specific case of the general dynamics presented in Sec. II, where feedback is triggered only in mode  $b_2$  from a photon detection in  $d_1$  and only in mode  $b_1$  from a photon detection in  $d_2$ . The aim of the scheme is to measure the phase difference  $\tilde{\varphi} = \varphi_1 - \varphi_2$  from the photon statistics in the detectors.

sense an unknown phase shift. In Section IV, we analyse the capabilities of our quantum jump metrology scheme and present numerical results. Finally, we summarise our findings in Section V.

## II. A TWO-MODE CAVITY NETWORK WITH QUANTUM FEEDBACK

In this Section, we review the main tools for the theoretical modelling of the experimental setup shown in Fig. 2. As we simply consider laser driving of optical cavities, the quantised electromagnetic field inside the resonators remains always in a coherent state. In the following we have a closer look at the dynamics of these coherent states under the condition of no photon emission and in case of an emission. In addition, we introduce quantum optical master equations which can be used for the prediction of ensemble expectation values.

### A. Multi-mode Coherent States and Transformation Matrices

As mentioned already above, in this paper we consider a network of two leaky optical cavities that are always kept in a coherent state. In Fock state representation, the coherent state  $|\gamma_i\rangle$  of cavity  $i$  can be solely parametrised by a complex number  $\gamma_i$  such that

$$|\gamma_i\rangle = \exp\left(-\frac{|\gamma_i|^2}{2}\right) \sum_{n_i=0}^{\infty} \frac{\gamma_i^{n_i}}{\sqrt{n_i!}} |n_i\rangle. \quad (4)$$

Here  $|n_i\rangle$  is the state with exactly  $n_i$  photons in cavity  $i$ . If  $c_i$  is the annihilation operator for a single photon in cavity  $i$ , then one can show that  $c_i |\gamma_i\rangle = \gamma_i |\gamma_i\rangle$ . Using this notation, the state  $|\psi(t)\rangle$  of both cavities at time  $t$

is always of the form

$$|\psi(t)\rangle = \bigotimes_{i=1,2} |\gamma_i(t)\rangle \quad (5)$$

and its dynamics can be modelled simply by tracking two complex numbers  $\gamma_i(t)$ . Hence we can also express the state of the two cavities as

$$\underline{\gamma}(t) = \begin{pmatrix} \gamma_1(t) \\ \gamma_2(t) \end{pmatrix}. \quad (6)$$

In the following, we adopt a vector and matrix notation for convenience when considering photon counting and quantum feedback processes.

The experimental setup in Fig. 2 contains phase shifters and beamsplitters. Hence quantum feedback pulses do not perturb the cavities directly. Similarly, photons arriving at a detector do not come directly from only a single cavity. To take this into account more easily, we denote the annihilation operator of the field mode seen by detector  $i$  in the following by  $a_i$  and the annihilation operator of the field mode affected by laser  $i$  by  $b_i$ . With respect to these alternative modes, the state  $|\psi(t)\rangle$  of the cavities is given by the complex vectors

$$\underline{\alpha}(t) = \begin{pmatrix} \alpha_1(t) \\ \alpha_2(t) \end{pmatrix}, \quad \underline{\beta}(t) = \begin{pmatrix} \beta_1(t) \\ \beta_2(t) \end{pmatrix} \quad (7)$$

with the complex numbers  $\alpha_i(t)$  and  $\beta_i(t)$  such that  $a_i |\alpha_i(t)\rangle = \alpha_i(t) |\alpha_i(t)\rangle$  and  $b_i |\beta_i(t)\rangle = \beta_i(t) |\beta_i(t)\rangle$ . To switch from one representation of the cavity network in Fig. 2 to another, we define transformation matrices  $M_{yx}$  with

$$\begin{pmatrix} y_1 \\ y_2 \end{pmatrix} = M_{yx} \begin{pmatrix} x_1 \\ x_2 \end{pmatrix}, \quad (8)$$

where  $x_i, y_i = \alpha_i(t), \beta_i(t), \gamma_i(t)$  and where  $x, y = a, b, c$ . Below we have a closer look at these matrices which depend on the effect of the beamsplitters and the phase

shifters shown in Fig. 2. If we define the transformation matrices

$$S_{BS} = \frac{1}{\sqrt{2}} \begin{pmatrix} 1 & i \\ i & 1 \end{pmatrix}, \quad S_{\varphi_1} = \begin{pmatrix} 1 & 0 \\ 0 & e^{i\varphi_1} \end{pmatrix},$$

$$S_{\varphi_2} = \begin{pmatrix} e^{i\varphi_2} & 0 \\ 0 & 1 \end{pmatrix}, \quad (9)$$

then one can now show that

$$M_{cb} = S_{\varphi_1} S_{BS} = \frac{1}{\sqrt{2}} \begin{pmatrix} 1 & i \\ i e^{i\varphi_1} & e^{i\varphi_1} \end{pmatrix},$$

$$M_{ac} = S_{BS} S_{\varphi_2} = \frac{1}{\sqrt{2}} \begin{pmatrix} e^{i\varphi_2} & i \\ i e^{i\varphi_2} & 1 \end{pmatrix}. \quad (10)$$

These matrices can be used to easily switch from one representation of the cavity state into another and to easily model the detection of photons, the no-photon time evolution and the effect of the quantum feedback pulses. For example,  $\underline{\alpha}(t) = M_{ac} \underline{\gamma}(t)$ .

### B. The effect of quantum feedback

Suppose an instantaneous strong laser pulse is applied directly to cavity  $i$ . Then the effect of this operation on the coherent state  $|\gamma_i(t)\rangle$  of cavity  $i$  can be described by a displacement operator of the form

$$D_i(\gamma) = \exp(\gamma c_i^\dagger - \gamma^* c_i) \quad (11)$$

where  $\gamma$  is a complex number. Taking this into account, one can show that the result is a change such that

$$\gamma_i(t) \rightarrow \gamma_i(t) + \gamma. \quad (12)$$

However, in the experimental setup in Fig. 2, quantum feedback pulses do not trigger a laser pulse that disturbs the cavities directly. Instead, because of the presence of a beamsplitter, each laser pulse usually affects the field in both cavities.

For simplicity, we take the feedback strengths of the laser pulses as constant in time, although it could be made time dependent for further generality. This allows us to model the effect of the feedback by four complex numbers  $\beta_i^{(d)}$  which characterise the quantum feedback strength generated by laser  $i$  upon detection of a photon in detector  $d$  with  $d = 1, 2$ . For convenience we arrange these numbers into two vectors

$$\underline{\beta}^{(d)} = \begin{pmatrix} \beta_1^{(d)} \\ \beta_2^{(d)} \end{pmatrix}. \quad (13)$$

Given that the feedback is triggered by the detection of a photon in detector  $d$ , we observe the following effect of quantum feedback on the state  $\underline{\gamma}(t)$  of the cavities,

$$\underline{\gamma}(t) \rightarrow \underline{\gamma}(t) + M_{cb} \underline{\beta}^{(d)}. \quad (14)$$

Alternatively, in the basis of the detector modes, the state of the cavities changes such that

$$\underline{\alpha}(t) \rightarrow \underline{\alpha}(t) + M_{ab} \underline{\beta}^{(d)} \quad (15)$$

with

$$M_{ab} = M_{ac} M_{cb} = \frac{1}{2} \begin{pmatrix} -e^{i\varphi_1} + e^{i\varphi_2} & i(e^{i\varphi_1} + e^{i\varphi_2}) \\ i(e^{i\varphi_1} + e^{i\varphi_2}) & e^{i\varphi_1} - e^{i\varphi_2} \end{pmatrix}. \quad (16)$$

This equation provides a complete description of the quantum feedback.

### C. Master equations and Quantum Jump Approach

Next we study the effect of the possible leakage of photons through the cavity mirrors on the state of the resonator fields. Because of the presence of spontaneous photon emission, the calculation of expectation values for ensemble averages requires the introduction of a density matrix  $\rho$ . In the absence of quantum feedback, this density matrix evolves such that

$$\dot{\rho} = \sum_{d=1,2} \kappa_d a_d \rho a_d^\dagger - \frac{1}{2} \kappa_d [a_d^\dagger a_d, \rho]_+, \quad (17)$$

where  $\kappa_d$  denotes the spontaneous decay rate of a single photon in the  $a_d$  mode. However, using the notation introduced above, one can show that this master equation changes into

$$\dot{\rho} = \sum_{d=1,2} \kappa_d D_2(\beta_2^{(d)}) D_1(\beta_1^{(d)}) a_d \rho a_d^\dagger D_1^\dagger(\beta_1^{(d)}) D_2^\dagger(\beta_2^{(d)})$$

$$- \frac{1}{2} \kappa_d [a_d^\dagger a_d, \rho]_+ \quad (18)$$

in the presence of quantum feedback with

$$D_i(\beta_i^{(d)}) = \exp(\beta_i^{(d)} b_i^\dagger - \beta_i^{(d)*} b_i). \quad (19)$$

Unfortunately, in general, it is not possible to find analytic solutions to this equation. In the following, we therefore have a closer look at an unravelling of the above ensemble dynamics into individual quantum trajectories. These are easier to study analytically, especially if the cavities are initially prepared in a pair coherent state given by  $\underline{\gamma}(0)$ .

#### 1. The no-photon time evolution

To obtain the conditional no-photon evolution, we write the master equation in Eq. (18) as

$$\dot{\rho} = \sum_{d=1,2} \kappa_d D_2(\beta_2^{(d)}) D_1(\beta_1^{(d)}) a_d \rho a_d^\dagger D_1^\dagger(\beta_1^{(d)}) D_2^\dagger(\beta_2^{(d)})$$

$$- \frac{i}{\hbar} [H_{\text{cond}}, \rho] \quad (20)$$

with the conditional Hamiltonian  $H_{\text{cond}}$  given by

$$H_{\text{cond}} = -\frac{i}{2}\hbar \sum_{d=1,2} \kappa_d a_d^\dagger a_d. \quad (21)$$

While the terms in the first line of the above equation describe subensembles of systems with a photon detection in output port  $d$ , the second line describes the subensemble without an emission. In other words, the non-Hermitian Hamiltonian  $H_{\text{cond}}$  is the generator for time evolution of the experimental setup in Fig. 2 conditioned on no photon emission. The corresponding time evolution operator

$$U_{\text{cond}}(t, 0) = \exp\left(-\frac{i}{\hbar} H_{\text{cond}} t\right) \quad (22)$$

reduces the norm of state vectors and can be used to calculate the probability  $P_{00}(t)$  for no photon detection in both detectors in a time interval  $(0, t)$  which equals

$$P_{00}(t) = \|U_{\text{cond}}(t, 0)|\psi(0)\rangle\|^2 \quad (23)$$

given the initial state  $|\psi(0)\rangle$ . For example, given an initial pair coherent state  $|\psi(0)\rangle = |\alpha_1\rangle |\alpha_2\rangle$  with respect to the modes  $a_1$  and  $a_2$  seen by the detector, one can show that

$$\begin{aligned} U_{\text{cond}}(t, 0) |\alpha_1\rangle |\alpha_2\rangle &= \exp\left(\frac{-|\alpha_1|^2}{2} (1 - e^{-\kappa_1 t})\right) \\ &\times \exp\left(\frac{-|\alpha_2|^2}{2} (1 - e^{-\kappa_2 t})\right) \\ &\times |\alpha_1 e^{-\frac{1}{2}\kappa_1 t}\rangle |\alpha_2 e^{-\frac{1}{2}\kappa_2 t}\rangle. \end{aligned} \quad (24)$$

Hence, using the notation introduced in Sec. II A, we can summarise the effect of the no-photon time evolution of the field inside the cavities as  $\underline{\alpha}(t) = M_0(t)\underline{\alpha}(0)$  with

$$M_{00}(t) = \begin{pmatrix} e^{-\frac{1}{2}\kappa_1 t} & 0 \\ 0 & e^{-\frac{1}{2}\kappa_2 t} \end{pmatrix}. \quad (25)$$

The probability of such an evolution occurring is

$$\begin{aligned} P_{00}(t) &= \exp[-|\alpha_1(t)|^2 (1 - e^{-\kappa_1 t})] \\ &\times \exp[-|\alpha_2(t)|^2 (1 - e^{-\kappa_2 t})], \end{aligned} \quad (26)$$

due to Eq. (23).

## 2. Photon emission probabilities

Next we calculate the probabilities of photon emission. Having a closer look at the factors in Eq. (26), we see that the probability for an individual detector mode  $i$  not to detect a photon equals

$$P_0^{(i)}(t) = \exp[-|\alpha_i(t)|^2 (1 - e^{-\kappa_i t})]. \quad (27)$$

Moreover, we know that the probability to find at least one photon in detector  $i$  is given by  $1 - P_0^{(i)}(t)$ . Thus the

probability for no photon in detector 1 and at least one photon in detector 2 equals

$$\begin{aligned} P_{01}(t) &= \exp[-|\alpha_1(t)|^2 (1 - e^{-\kappa_1 t})] \\ &\times (1 - \exp[-|\alpha_2(t)|^2 (1 - e^{-\kappa_2 t})]). \end{aligned} \quad (28)$$

Analogously,

$$\begin{aligned} P_{10}(t) &= (1 - \exp[-|\alpha_1(t)|^2 (1 - e^{-\kappa_1 t})]) \\ &\times \exp[-|\alpha_2(t)|^2 (1 - e^{-\kappa_2 t})] \end{aligned} \quad (29)$$

is the probability for at least one photon in detector 1 and no photon in detector 2. To cover all possibilities, we should also consider the probability

$$\begin{aligned} P_{11}(t) &= (1 - \exp[-|\alpha_1(t)|^2 (1 - e^{-\kappa_1 t})]) \\ &\times (1 - \exp[-|\alpha_2(t)|^2 (1 - e^{-\kappa_2 t})]) \end{aligned} \quad (30)$$

for the case in which at least one photon has been emitted into both detector modes.

For relatively short time intervals  $\Delta t$  such that the presence of two photons in one detector becomes negligible and the probabilities  $P_{01}(\Delta t)$ ,  $P_{10}(\Delta t)$  and  $P_{11}(\Delta t)$  become the probabilities to have exactly one photon in mode 2, exactly one photon in mode 1 and exactly one photon in each mode, respectively. In this case, the corresponding changes of the state vector  $\underline{\alpha}(0)$  of the cavity fields can be described by transformation operators  $M_{ij}(\Delta t)$  such that  $\underline{\alpha}(t) = M_{ij}(\Delta t)\underline{\alpha}(0)$ . To a very good approximation, the  $M_{ij}(\Delta t)$  are given by

$$\begin{aligned} M_{01}(\Delta t) \underline{\alpha}(0) &= M_{00}(\Delta t) (\underline{\alpha}(0) + \underline{\beta}^{(2)}) \\ M_{10}(\Delta t) \underline{\alpha}(0) &= M_{00}(\Delta t) (\underline{\alpha}(0) + \underline{\beta}^{(1)}) \\ M_{11}(\Delta t) \underline{\alpha}(0) &= M_{00}(\Delta t) (\underline{\alpha}(0) + \underline{\beta}^{(1)} + \underline{\beta}^{(2)}) \end{aligned} \quad (31)$$

with  $M_{00}(\Delta t)$  given in Eq. (25). We now have a complete toolbox for modelling quantum trajectories within this system through piecewise evolution of the system, as suggested by standard quantum jump methods [49–51].

## III. GENERAL DYNAMICS AND TEMPORAL CORRELATIONS

In this section, we study the behaviour of the experimental setup in Fig. 2 in more detail to understand better, how it can be used to perform measurements of the phase  $\tilde{\varphi} = \varphi_1 - \varphi_2$ . We then consider the fundamental limits of the measurement accuracy that we can expect for the proposed cavity network.

### A. Dynamics and Quantum trajectories

In the proceeding discussions we analyse the behaviour and the sensing capabilities of the cavity network shown

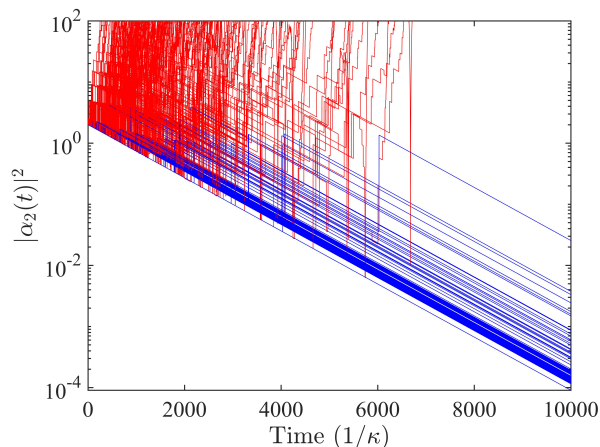


FIG. 3: Illustration of the dynamics of the state  $\underline{\alpha}(t)$  of the two cavities in the detector mode basis. Here we present 500 individual trajectories for initial parameters  $\gamma_1(0) = \gamma_2(0) = 1$ , quantum feedback as described by Eq. (32) with  $\beta_2^{(1)} = 1$  and  $\beta_1^{(2)} = 2$ ,  $\kappa_1 = \kappa_2 = \kappa$ ,  $\Delta t = 10^{-3}\kappa^{-1}$  and  $\tilde{\varphi} = 0$ . We show the population  $|\alpha_2(t)|^2$  of the detector mode  $a_2$  as a function of time in semi-log scale. It is clear to see the difference in behaviour, as some trajectories diverge, while others decay towards the vacuum, as signified by the different line shades.

in Fig. 2 for a specific example of quantum feedback, which can be described by

$$\underline{\beta}^{(1)} = \begin{pmatrix} 0 \\ \beta_2^{(1)} \end{pmatrix} \quad \underline{\beta}^{(2)} = \begin{pmatrix} \beta_1^{(2)} \\ 0 \end{pmatrix}. \quad (32)$$

As pointed out already in the previous section, we treat the quantum feedback as approximately instantaneous. For simplicity, we also consider the case of perfect photon detection and assume that all photons are counted and trigger feedback pulses. Losses could be incorporated but do not largely effect the overall behaviour of the cavity network and are therefore neglected here [35]

Although the experimental setup that we analyse in this paper remains always in a coherent state, its dynamics are nevertheless complex due to the action of the quantum feedback. While optical cavities with continuous laser driving smoothly evolves into a steady state, the same does not always apply in the presence of quantum feedback. For example, when the feedback is in the form of strong laser pulses, the free decay of the cavity field is perturbed by ‘kicks’ to the dynamics. These kicks occur the more often, the more photons are inside the resonator and hence result into a divergence of the average photon number inside the cavity. This highly non-linear behaviour prevents us from obtaining a straightforward closed analytic solution to the master equation and its statistical moments, despite the cavities always being in a coherent state.

Considering the individual quantum trajectories of the system in Fig. 3 reveals subtle behaviour. In particular, we see the creation of two types of dynamics. In one case

we see a divergence of cavity photon numbers, with each feedback pulse making the state even more likely to emit a photon and thus diverging further due to subsequent feedback pulses. However, we also see trajectories that do not follow this evolution and decay towards the vacuum state, with only a small number of photon emissions. Generally, after a reasonable amount of time has passed, trajectories do not swap behaviour and clearly belong to one of two subensembles, which leads to effective ergodicity breaking [46].

Let us emphasise here that this behaviour emerges as a result of manipulating quantum trajectories and as such is not reproducible classically. To see this, try to consider a “classical analogue” to the experimental setup shown in Fig. 2. For example, an optical cavity could have the output intensity monitored. Then, based upon the measured intensity, feedback could be applied. However, this would lead to a well defined evolution of the dynamics that would not vary over multiple trajectories. As such, the above described generation of individual stochastic trajectories is a truly quantum feature. Measurements depending on this quantum feature will be capable of showing non-classical correlations [52, 53]. It is this property that we exploit in this work to develop a quantum jump metrology scheme [35, 36]. In order to see how this quantum enhancement manifests, we now proceed to more precisely consider the limits of measurement precision.

## B. Quantum Jump Metrology

The amount of information that can be gained from a measurement is quantified by the Fisher information. Let  $\mathbf{x}$  be a string of data of length  $N$  with elements  $x_i \in \mathbb{Z}^+$ . The Fisher information for such data is defined as

$$\begin{aligned} F(P_\varphi) &\equiv \sum_{x_i} P(\mathbf{x}) [\partial_\varphi \ln(P_\varphi(\mathbf{x}))]^2 \\ &= \sum_{x_i} \frac{[\partial_\varphi P_\varphi(\mathbf{x})]^2}{P_\varphi(\mathbf{x})}. \end{aligned} \quad (33)$$

Here  $\varphi$  is the unknown parameter to be probed, which the probability distribution must hence be a function of. We sum over all possible combinations of output data  $\mathbf{x}$ . Now let  $\hat{\varphi}$  be an estimator of the unknown parameter  $\varphi$ . The Cramér-Rao bound tells us that the minimum uncertainty achievable by such an estimator is bounded by the Fisher information as

$$(\Delta\hat{\varphi})^2 \geq \frac{1}{F(P_\varphi)}. \quad (34)$$

If the  $N$  data points are uncorrelated, each contributes an independent amount of information such that  $(\Delta\hat{\varphi})^2$  scales like Eq. (1). If the generation of the data is repeated  $M$  times, and each repetition is statistically inde-

pendent of the others, then by the same logic

$$(\Delta\hat{\varphi})^2 \propto \frac{1}{MN}. \quad (35)$$

As one would expect, obtaining more data (through repetitions or larger sources) leads to a reduction in the uncertainty of the unknown parameter.

If however the data possesses correlations, then the information contribution from each value may now be beyond linear with respect to the number of data points. In particular, the correlations that may exist in quantum systems can lead to more precise measurements when compared with a classical system with the same number of particles [11–13]. With maximal correlations, such as in maximally entangled quantum states, the quantum Cramér-Rao bound tells us

$$(\Delta\hat{\varphi})^2 \propto \frac{1}{MN^2}. \quad (36)$$

Different ways of obtaining such enhancements have been thoroughly explored in recent years [54], such as through entanglement [14], squeezing [15] and phase transitions [55]. Unfortunately, while the theory predicts great results, achieving such feats experimentally is more difficult, due to the challenges in implementing quantum physics with more than a handful of particles. Another way of improving the limit of scaling within the system is with non-linear or interacting systems [30]. Such systems are capable of producing scaling of

$$(\Delta\hat{\varphi})^2 \propto \frac{1}{MN^k}, \quad (37)$$

where  $k$  is the order of the non-linearity or interaction. Such systems have been shown to be capable of producing very good scaling [30], but again are typically hard to implement experimentally.

However, a quantum jump provides a non-linearity in the dynamics of a quantum trajectory and thus a measurement that explicitly depends on the properties of trajectories instead of depending on ensemble averages has already been shown to be capable of enhanced measurements [35, 36]. To see this, consider the time evolution of an open quantum system described by a density matrix  $\rho$ , which can be expressed by the standard Lindbladian master equation

$$\dot{\rho} = -\frac{i}{\hbar} [H, \rho] + \Gamma \left( L\rho L^\dagger - \frac{1}{2} [L^\dagger L, \rho]_+ \right) \quad (38)$$

with Hamiltonian  $H$  and where for simplicity we have considered a single decay channel with Lindblad operator  $L$  and rate  $\Gamma$ . Clearly, this equation is linear. However, the evolution of a trajectory may follow a stochastic master equation of the form

$$\begin{aligned} d\rho = & \left( -\frac{i}{\hbar} [H, \rho] - \frac{\Gamma}{2} [L^\dagger L, \rho]_+ + \text{Tr}(L^\dagger L \rho) \rho \right) dt \\ & + \left( \frac{L\rho L^\dagger}{\text{Tr}(L^\dagger L \rho)} - \rho \right) dN_t, \end{aligned} \quad (39)$$

with Poisson increment  $dN_t$  being zero for no-emission at time  $t$  or one in the case of an emission [56]. From Eq. (39) it is clear that the time evolution along an individual quantum trajectory is non-linear in general, so long as quantum jumps exist and  $L\rho L^\dagger \neq \rho$ . Clearly, if  $\rho$  is a coherent state and  $L$  is simply the annihilation operator, this is not the case and as such there will be no quantum enhancement. This shows why feedback is necessary and how it hence induces quantum enhancements to sensing performance. Therefore, if the quantum jump depends on the parameter to be measured in some way, a quantum-enhanced measurement may be possible.

Here we study the bath statistics of an open quantum system in order to extract information about an unknown internal system parameter, such as a phase  $\varphi$ . If the emission of quanta from the system to the bath creates a quantum jump within the dynamics of the system, temporal correlations may exist in the bath, which may allow for enhanced measurement sensitivity [35, 36]. It is straightforward to see that such correlations exist. Consider an open quantum system whose dynamics can be described by a set of Kraus operators  $K_x$  with

$$\sum_x K_x^\dagger K_x = \mathbb{1}. \quad (40)$$

Let  $\rho$  be a density matrix describing the internal state of an open quantum system. Then upon the measurement of  $x$  in the bath, the internal state of the system evolves to  $\rho \rightarrow K_x \rho K_x^\dagger$ . This state is unnormalised, occurring with probability  $\text{Tr}[K_x \rho K_x^\dagger]$ . Now consider a series of  $N$  measurements of  $\{x_i\}_{i=1}^N$ . The resulting density matrix occurs with probability

$$p(x_1, \dots, x_N) = \text{Tr} \left[ \left( \prod_{i=1}^N K_{x_{N+1-i}} \right) \rho \left( \prod_{i=1}^N K_{x_i}^\dagger \right) \right]. \quad (41)$$

The Kraus operators  $K_x$  do not necessarily commute, thus the events and measurements are not independent from one another. This can be seen more clearly by comparing the probabilities

$$p(x_N | x_{N-1}) = \frac{\text{Tr} [K_N K_{N-1} \mathcal{T}_1^{N-2}(\rho) K_{N-1}^\dagger K_N^\dagger]}{\text{Tr} [K_{N-1} \mathcal{T}_1^{N-2}(\rho) K_{N-1}^\dagger]}, \quad (42)$$

which is the probability of measuring  $x_N$  after  $x_{N-1}$  in the previous time step with the probability of measuring  $x_N$  after  $x_{N-1}$  and  $x_{N-2}$

$$\begin{aligned} p(x_N | x_{N-1} x_{N-2}) &= \frac{\text{Tr} [K_N K_{N-1} K_{N-2} \mathcal{T}_1^{N-3}(\rho) K_{N-2}^\dagger K_{N-1}^\dagger K_N^\dagger]}{\text{Tr} [K_{N-1} K_{N-2} \mathcal{T}_1^{N-3}(\rho) K_{N-2}^\dagger K_{N-1}^\dagger]}. \end{aligned} \quad (43)$$



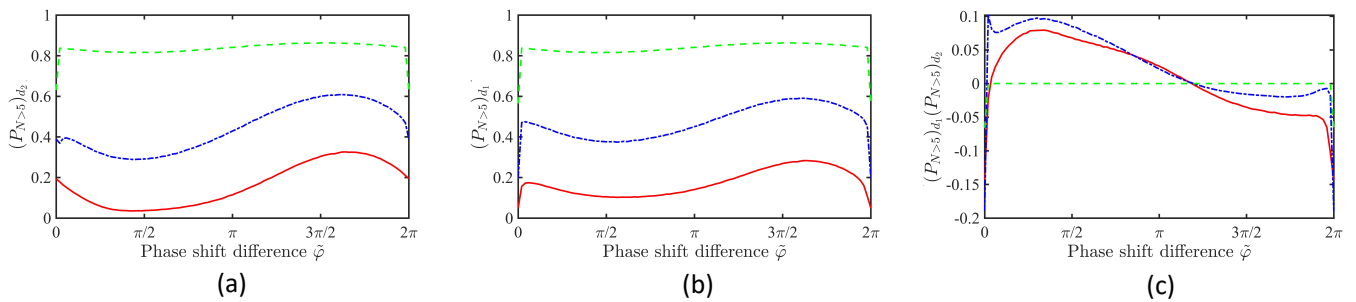


FIG. 4: The probability  $(P_{N>5})_{d_i}$  of surpassing the threshold number of  $N = 5$  photon emissions within a certain time interval  $(0, t)$  as a function of the phase shift difference  $\tilde{\varphi}$  for  $t = 0.5 \kappa^{-1}$  (red-solid),  $t = \kappa^{-1}$  (blue-dot-dashed) and  $t = 10 \kappa^{-1}$  (green-dashed). Here we average over  $10^4$  trajectories with  $\Delta t = 10^{-3} \kappa^{-1}$ ,  $\gamma_1(0) = \gamma_2(0) = 1$  and quantum feedback as described in Eq. (32) with  $\beta_1^{(2)} = 2$  and  $\beta_2^{(1)} = 1$ . The figure shows (a)  $(P_{N>5})_{d_2}$ , (b)  $(P_{N>5})_{d_1}$  and (c)  $(P_{N>5})_{d_1} - (P_{N>5})_{d_2}$  as a function of  $\tilde{\varphi}$ .

The superoperator  $\mathcal{T}_i^j$  describes a Markovian evolution from time-step  $i$  to  $j$ . In general, Eqs. (42) and (43) differ, meaning the measurement statistics do not form a Markov chain and thus possess correlations [35, 36]. If the Kraus operators are dependent on the unknown parameter, these correlations may lead to a Fisher information growing faster than linearly and thus allows for enhanced precision. As we shall see below, in the case of the cavity network with quantum feedback that we consider here, this is the case and thus the potential for obtaining quantum enhanced measurements exists.

#### IV. A SIMPLE MEASUREMENT SCHEME FOR ESTIMATING PHASE DIFFERENCE

In this section, we finally discuss, how the phase difference  $\tilde{\varphi} = \varphi_1 - \varphi_2$  between two pathways of the network shown in Fig. 2 can be measured. We propose a simple experimental scheme and analyse its performance by calculating the uncertainty of  $\tilde{\varphi}$  based on an ensemble of simulated quantum trajectories.

##### A. The basic protocol

As Fig. 3 shows, there are two classes of trajectory. Moreover, it shows that the relative size of the subensemble associated with each class has a relatively strong dependence on the phase difference  $\tilde{\varphi}$  that we want to estimate. This applies since the only way that energy is put into the system is through quantum feedback, which is triggered upon photon emission. The number of detected photons therefore acts as a reliable signal for the type of trajectory being observed. For example, a convergent trajectory will have emitted no or few photons until a given time  $t$ , whereas an eventually divergent one is likely to have emitted many photons due to the repeated pumping of energy into the system. In the following, we therefore take the probability of the total number of

emitted photons until a given time  $t$  surpassing a certain threshold  $N$  as our measurement signal. In particular, we take the probability of the number of photons surpassing 5 as our signal, denoted as  $P_{N>5}$ . This signal is a good indicator of which trajectory class the system is following. However, it is important to choose the parameters carefully in order to ensure the signal reveals useful information. For example, choosing the threshold number of photons to be too low won't faithfully distinguish between the trajectory classes, depending also on the strength of the feedback and size of the initial state. Therefore, finding a balance between these is essential when determining the phase difference  $\tilde{\varphi}$ .

As mentioned in the previous section, an analytic calculation for the behaviour of the ensemble is straightforward due to the quantum feedback giving rise to non-linear dynamics. Hence, to determine the uncertainty of the estimator of  $\tilde{\varphi}$ , we numerically simulate a large number of trajectories over a coarse-grained timescale. By sampling these trajectories, we are able to estimate the probability of the system emitting a number of photons surpassing the threshold we set. From this, we then infer the uncertainty of measuring  $\tilde{\varphi}$  from this data as a function of the time  $t$ .

##### B. Measurement of phase difference

Here we consider a specific set of parameters to demonstrate the utility of our system for estimating a phase in an optical cavity network. As with the threshold value, it is important to choose feedback parameters that are both not too small and not too big. For example, for very weak feedback, we are unlikely to deduce information about  $\tilde{\varphi}$  over reasonable timescales. Moreover, for very strong feedback, the dynamics of the cavity network becomes dominated by the feedback, almost all trajectories diverge and the measurement outcomes are essentially independent of the unknown phase that we want to identify. Finally, in order to avoid starting in the vac-



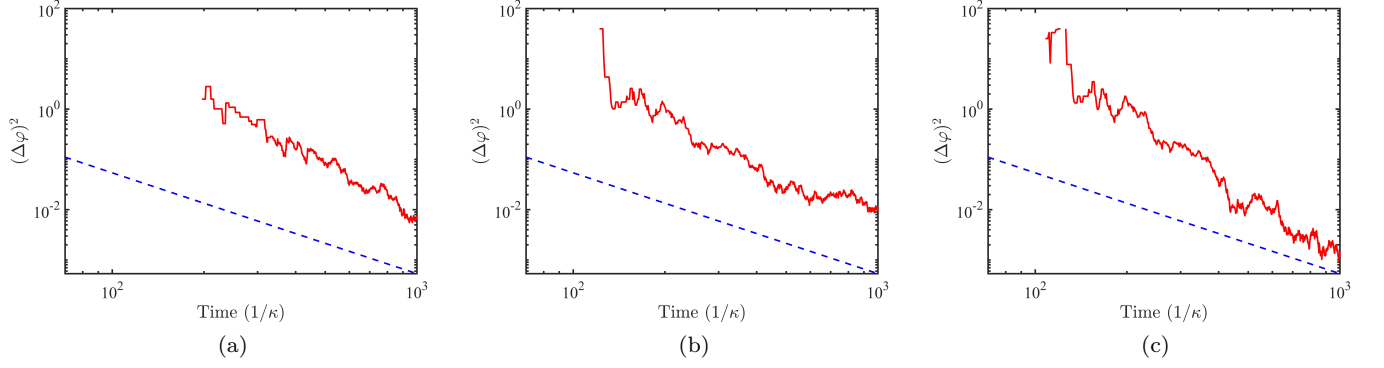


FIG. 5: The uncertainty in the phase shift measurement for phase differences  $\tilde{\varphi} = \pi/10$  as function of time is shown for the solid line. The probabilities shown in Fig. 4 are generated with  $10^3$  trajectories and 10 subensembles of these are generated to obtain the variance of the estimator. The dashed line shows the extrapolated value of the reciprocal of the Fisher information, providing an estimated lower bound on potential the sensitivity of the data. The Fisher information is obtained exactly for 12 time steps  $\Delta t$  and the subsequent fit is extended for all time. We plot the data of our results only for later times, where the trend is clearer to see. All parameters are as in Fig. 4.

uum state and for the practicality of implementation, we start each trajectory with a feedback pulse to prepare a non-trivial initial state. With all of these factors in mind, Fig. 4 shows three different measurement signals obtained after three different times  $t$ . Three different observables are considered, namely, the probabilities  $(P_{N>5})_{d_1}$  and  $(P_{N>5})_{d_2}$  and their difference  $(P_{N>5})_{d_1} - (P_{N>5})_{d_2}$ . All three observables can be used to infer the value of  $\tilde{\varphi}$ .

As we shall see below, considering only the output of either of the detectors, i.e. considering only  $(P_{N>5})_{d_1}$  or  $(P_{N>5})_{d_2}$ , does not give the best sensitivity since some of the available information from the dynamics of the system is omitted in this case. It is better to take information from both detectors into account and to use instead  $(P_{N>5})_{d_1} - (P_{N>5})_{d_2}$  as the estimator for  $\tilde{\varphi}$ . To show that this is indeed the case, we now determine the measurement uncertainty  $\delta\tilde{\varphi}$  with the help of the standard error propagation formula

$$(\Delta\varphi)^2 = \frac{(\Delta O)^2}{\left| \frac{\partial \langle O \rangle}{\partial \varphi} \right|^2}, \quad (44)$$

where  $O$  denotes the relevant observable. The variance in the numerator of this equation is obtained by sampling over a number of subensembles of trajectories, while the visibility in the denominator is obtained numerically from Fig. 4. The result of this calculation is shown in Fig. 5. As in Fig. 4, three different observables are considered. Our results show that as time increases we obtain better accuracy for measuring the phase shift  $\tilde{\varphi}$  in either detector mode. However, we obtain our best results when we consider the difference between the two threshold probabilities  $(P_{N>5})_{d_1}$  and  $(P_{N>5})_{d_2}$ .

Considering Fig. 4, we see that the optimal phase to conduct an estimation at is around  $\tilde{\varphi} = 0$  due to the sharpness of the gradient at this point. This corresponds to a crucial point in the dynamics. When  $\tilde{\varphi} = 0$ , only one

detector mode is ever occupied. However, moving away from this point, the other detector mode begins to be occupied too. Thus, taking advantage of this distinction in the signal allows for the best measurement. Due to numerical instabilities evaluating at this point however, we take our data at a nearby value of  $\tilde{\varphi} = \pi/10$ , where the gradient is still large for reasonable amounts of time.

### C. Fisher information for the photon statistics of an optical cavity network

Finally, we calculate the Fisher information of the photon statistics using the methods outlined in Section III B in order to obtain a bound on the optimum precision our measurement scheme can achieve. The probability of a certain trajectory with a given number of time steps can be calculated using Eq. (41). To do so, it has to be taken into account that every individual time step has one of four different possible event types (no-photon, photon in a single detector or photons in both detectors). The theoretical model to describe each of these events has been introduced in Section II. A drawback of this however is that an exact calculation of the Fisher information for a trajectory of length  $N$  requires summing over  $4^N$  trajectories. Hence this approach becomes computationally very challenging for large  $N$ . Nevertheless, as illustrated in Fig. 5, for small  $N$ , we find scaling beyond linear, of the form  $F(N) \propto N^2 - N$ . This result is in agreement with the scaling behaviour observed in Ref. [36], thus demonstrating the presence of correlations in the photon statistics that depend on  $\tilde{\varphi}$ .

The limitation of only having exact results for the Fisher information for a small number of time steps means we do not always have a strict bound for the system. Instead, we extrapolate the scaling shown for short times. We expect that this will be an upper bound

on the Fisher information, as it is likely that at large times the scaling will reduce rather than increase due to a breakdown in correlations between far away time steps. This estimated bound can nevertheless be useful for comparing to the uncertainty of our proposed measurement scheme though, as illustrated above in Fig. 4. In particular, the sensing performance in Fig. 5(c) approaches our extrapolated bound, thus suggesting that our fit result is reasonable.

## V. CONCLUSIONS

In this paper we have demonstrated how the phase difference between the “arms” of an optical cavity network (c.f. Fig. 2) can be inferred requiring only single photon detectors and quantum feedback in the form of strong but approximately instantaneous laser pulses. Despite the simplicity of the proposed measurement scheme, we have shown that it is capable of measuring the phase difference with a sensitivity beyond the standard quantum limit. As in previous work [35, 36], the presence of quantum jumps in the form of photon emissions is continuously monitored. Subsequent driving of the cavities creates non-linearities in the system dynamics, thereby inducing correlations in the photon statistics observed by the detectors.

In the experimental setup that we consider here, the cavities remain always in a coherent state. Although photon emission does not alter the state of the cavities, it reveals information about the state of the resonators. Similarly, not observing photons reveals information. The dependence of the quantum feedback induced dynamics on the parameter that we want to measure leads to effective ergodicity-breaking in the dynamics of the system, similar to the ergodicity breaking discussed in Ref. [46] and results in two different classes of trajectory. In this paper, we have shown that measuring the probability for these two classes of dynamics to occur reveal information about the phase difference between the arms of the cavity network beyond the standard quantum limit. Even better scaling might be achieved by preparing the cavities in a more complex initial state than a coherent state. However, the use of coherent states offers experimental simplicity and as such the proposed scheme can be operated more straightforwardly and for longer periods of time.

A limitation of our work is that the results are only attainable numerically, and the Fisher information is only calculable for small times. However, the expected behaviour has been predicted with approximations previously and the observed behaviour here is in line with this [46]. Moreover, it may be possible to obtain estimates for the Fisher information at large times by using sampling techniques. Even in this case however, the number of possible trajectories is extremely large even for reasonable values of  $N$ , thus meaning the number of trajectories needed to sample over may also need to be large. Due to how well the predicted bound matches the uncertainty predicted from our measurement signal though, we believe that our fitting of the Fisher information to be reasonable.

An alternative measurement protocol for gaining information about the phase would be to utilise all information gained in the continuous monitoring of the cavity network and follow a Bayesian inference procedure. In an open system where the photon statistics are observed this is perhaps the most natural way to envisage the measurement of an unknown parameter [57]. This could be further supplemented by a strong quantum measurement of the cavity state at the end of the observation which supplements the information gained from monitoring the photon statistics. For the purpose of this work though, we choose to just consider the Fisher information as a proof-of-principle that a quantum enhancement exists. Because of this property, cavity networks like the one shown in Fig. 2 are very likely to attract more attention for applications in quantum sensing and might play a crucial role in the development of quantum machine learning devices.

## Acknowledgements

LAC acknowledges support from the Foundation for Polish Science within the “Quantum Optical Technologies” project carried out within the International Research Agendas programme co-financed by the European Union under the European Regional Development Fund. KAR acknowledges the support from the Ministry of Higher Education, Research and Innovation in the Sultanate of Oman funded by The National Postgraduate Scholarship Programme.

- 
- [1] A. Crespi, M. Lobino, J. C. F. Matthews, A. Politi, C. R. Neal, R. Ramponi, R. Osellame and J. L. O’Brien, *Measuring protein concentration with entangled photons*, Appl. Phys. Lett. **100**, 233704 (2012).
  - [2] F. Wolfgramm, C. Vitelli, F. A. Beduini, N. Godbout and M. W. Mitchell, *Entanglement-enhanced probing of a delicate material system*, Nature Photon. **7**, 28 (2013).
  - [3] M. A. Taylor, J. Janousek, V. Daria, J. Knittel, B. Hage, H.-A. Bachor and W. P. Bowen, *Biological measurement beyond the quantum limit*, Nature Photon. **7**, 229 (2013).
  - [4] B. P. Abbott *et al.* (LIGO Scientific Collaboration and Virgo Collaboration), *Observation of Gravitational Waves from a Binary Black Hole Merger*, Phys. Rev. Lett. **116**, 061102 (2016).
  - [5] S. Aaronson and A. Arkhipov, *The computational complexity of linear optics*. In Proceedings of the forty-third

- annual ACM symposium on Theory of computing (pp. 333-342). ACM. (2011).
- [6] R. Loughridge and D. Y. Abramovitch, *A tutorial on laser interferometry for precision measurements*, 2013 American Control Conference, pp. 3686-3703 (2013). doi: 10.1109/ACC.2013.6580402.
  - [7] R. Demkowicz-Dobrzanski, M. Jarzyna and J. Kolodynski, *Quantum limits in optical interferometry*, Progress in Optics **60**, 345 (2015).
  - [8] Z. Blanco-Garcia, *Quantum Control of the States of Light in a Mach-Zehnder Interferometer*, J. Phys.: Conf. Ser. **839**, 012021 (2017).
  - [9] S. Yang and G. Zhang, *A review of interferometry for geometric measurement*, Meas. Sci. Technol. **29**, 102001 (2018).
  - [10] S. Ataman, A. Preda and R. Ionicioiu, *Phase sensitivity of a Mach-Zehnder interferometer with single-intensity and difference-intensity detection*, Phys. Rev. A **98**, 043856 (2018).
  - [11] V. Giovannetti, S. Lloyd and L. Maccone, *Quantum-Enhanced Measurements: Beating the Standard Quantum Limit*, Science **306**, 1330 (2004).
  - [12] V. Giovannetti, S. Lloyd and L. Maccone, *Quantum metrology*, Phys. Rev. Lett. **96**, 010401 (2006).
  - [13] V. Giovannetti, S. Lloyd and L. Maccone, *Advances in quantum metrology*, Nat. Photon. **5**, 222 (2011).
  - [14] C. M. Caves, *Quantum-mechanical noise in an interferometer*, Phys. Rev. D **23**, 1693 (1981).
  - [15] R. S. Bondurant and J. H. Shapiro, *Squeezed states in phase-sensing interferometers*, Phys. Rev. D **30**, 2548 (1984).
  - [16] M. J. Holland and K. Burnett, *Interferometric detection of optical phase shifts at the Heisenberg limit*, Phys. Rev. Lett. **71**, 1355 (1993).
  - [17] D. W. Berry and H. M. Wiseman, *Optimal states and almost optimal adaptive measurements for quantum interferometry*, Phys. Rev. Lett. **85**, 5098 (2000).
  - [18] T. Nagata, R. Okamoto, J. L. O'Brien, K. Sasaki and S. Takeuchi, *Beating the standard quantum limit with four-entangled photons*, Science **316**, 726 (2007).
  - [19] J. P. Dowling, *Quantum optical metrology — The low-down on high-NOON states*, Contemp. Phys. **49**, 125 (2008).
  - [20] I. Afek, O. Ambar, and Y. Silberberg, *High-NOON states by mixing quantum and classical light*, Science **328**, 879 (2010).
  - [21] G. Y. Xiang, B. L. Higgins, D. W. Berry, H. M. Wiseman and G. J. Pryde, *Entanglement-enhanced measurement of a completely unknown optical phase*, Nat. Photon. **5**, 43 (2011).
  - [22] M. D. Vidrighin, G. Donati, M. G. Genoni, X.M. Jin, W. S. Kolthammer, M. S. Kim and I. A. Walmsley, *Joint estimation of phase and phase diffusion for quantum metrology*, Nat. Comm. **5**, 1 (2014).
  - [23] H. Lee, P. Kok and J. P. Dowling, *A quantum Rosetta stone for interferometry*, J. Mod. Opt. **49**, 2325 (2002).
  - [24] M. W. Mitchell, J. S. Lundeen and A. M. Steinberg, *Super-resolving phase measurements with a multiphoton entangled state*, Nature **429**, 161 (2004).
  - [25] G. J. Pryde and A. G. White, *Creation of maximally entangled photon-number states using optical fiber multiports*, Phys. Rev. A **68**, 052315 (2003).
  - [26] Y. Israel, I. Afek, S. Rosen, O. Ambar and Y. Silberberg, *Experimental tomography of NOON states with large photon numbers*, Phys. Rev. A **85**, 022115 (2012).
  - [27] G. Gilbert, M. Hamrick and Y. S. Weinstein, *Practical quantum interferometry using photonic NOON states*, In Quantum Information and Computation V (Vol. **6573**, p. 65730K), International Society for Optics and Photonics (2007).
  - [28] N. Thomas-Peter, B. J. Smith, A. Datta, L. Zhang, U. Dorner and I. A. Walmsley, *Real-world quantum sensors: evaluating resources for precision measurement*, Phys. Rev. Lett. **107**, 113603 (2011).
  - [29] B. L. Higgins, D. W. Berry, S. D. Bartlett, H. M. Wiseman and G. J. Pryde, *Entanglement-free Heisenberg-limited phase estimation*, Nature **450**, 393 (2007).
  - [30] S. Boixo, A. Datta, S. T. Flammia, A. Shaji, E. Bagan and C. M. Caves, *Quantum-limited metrology with product states*, Phys. Rev. A **77**, 012317 (2008).
  - [31] S. Boixo, A. Datta, M. J. Davis, S. T. Flammia, A. Shaji and C. M. Caves, *Quantum metrology: dynamics versus entanglement*, Phys. Rev. Lett. **101**, 040403 (2008).
  - [32] M. Napolitano, M. Koschorreck, B. Dubost, N. Behbood, R. J. Sewell and M. W. Mitchell, *Interaction-based quantum metrology showing scaling beyond the Heisenberg limit*, Nature **471**, 486 (2011).
  - [33] A. Datta and A. Shaji, *Quantum metrology without quantum entanglement*, Mod. Phys. Lett. B **26**, 1230010 (2012).
  - [34] D. Braun, G. Adesso, F. Benatti, R. Floreanini, U. Marzolino, M. W. Mitchell and S. Pirandola, *Quantum-enhanced measurements without entanglement*, Rev. Mod. Phys. **90**, 035006 (2018).
  - [35] L. A. Clark, A. Stokes and A. Beige, *Quantum-enhanced metrology with the single-mode coherent states of an optical cavity inside a quantum feedback loop*, Phys. Rev. A **94**, 023840 (2016).
  - [36] L. A. Clark, A. Stokes and A. Beige, *Quantum jump metrology*, Phys. Rev. A **99**, 022102 (2019).
  - [37] H. M. Wiseman and G. J. Milburn, *Quantum measurement and control*, Cambridge University Press (2009).
  - [38] A. Shabani, J. Roden and K. B. Whaley, *Continuous measurement of a non-Markovian open quantum system*, Phys. Rev. Lett. **112**, 113601 (2014).
  - [39] J. F. Haase, A. Smirne, S. F. Huelga, J. Kolodynski and R. Demkowicz-Dobrzanski, *Precision limits in quantum metrology with open quantum systems*, Quantum Meas. Quantum Metrol. **5**, 13 (2016).
  - [40] M. Beau and A. del Campo, *Nonlinear quantum metrology of many-body open systems*, Phys. Rev. Lett. **119**, 010403 (2017).
  - [41] F. Albarelli, M. A. Rossi, D. Tamascelli and M. G. Genoni, *Restoring Heisenberg scaling in noisy quantum metrology by monitoring the environment*, Quantum **2**, 110 (2018).
  - [42] C. Ahn, A. C. Doherty and A. J. Landahl, *Continuous quantum error correction via quantum feedback control*, Phys. Rev. A **65**, 042301 (2002).
  - [43] J. Wang and H. M. Wiseman, *Feedback-stabilization of an arbitrary pure state of a two-level atom*, Phys. Rev. A **64**, 063810 (2001).
  - [44] J. Wang, H. M. Wiseman and G. J. Milburn, *Dynamical creation of entanglement by homodyne-mediated feedback*, Phys. Rev. A **71**, 042309 (2005).
  - [45] L. A. Clark, W. Huang, T. Barlow and A. Beige, *Hidden Quantum Markov Models and Open Quantum Systems with Instantaneous Feedback*. In ISCS 2014: Interdisci-

- plinary Symposium on Complex Systems (pp. 143-151). Springer, Cham. (2015).
- [46] L. A. Clark, F. Torzewska, B. Maybee and A. Beige, *Non-ergodicity in open quantum systems through quantum feedback*, EPL **130**, 54002 (2020).
  - [47] G. K. Gulati, H. Takahashi, N. Podoliak, P. Horak and M. Keller, *Fiber cavities with integrated mode matching optics*, Sci. Rep. **7**, 5556 (2017).
  - [48] I. E. Zadeh *et al.*, *Efficient single-photon detection with 7.7 ps time resolution for photon-correlation measurements*, ACS Photonics **7**, 1780 (2020).
  - [49] G. C. Hegerfeldt, *How to reset an atom after a photon detection: Applications to photon-counting processes*, Phys. Rev. A **47**, 449 (1993).
  - [50] J. Dalibard, Y. Castin and K. Mølmer, *Wave-function approach to dissipative processes in quantum optics*, Phys. Rev. Lett. **68**, 580 (1992).
  - [51] H. Carmichael, *An Open Systems Approach to Quantum Optics*, Lecture Notes in Physics, Volume **18** (Springer, Berlin, 1993).
  - [52] A. Monras, A. Beige and K. Wiesner, *Hidden Quantum Markov Models and non-adaptive read-out of many-body states*, Appl. Math. and Comp. Sciences **3**, 93 (2011); arXiv:1002.2337.
  - [53] L. A. Clark, W. Huang, T. M. Barlow and A. Beige, *Hidden Quantum Markov Models and Open Quantum Systems with Instantaneous Feedback*, ISCS 2014: Interdisciplinary Symposium on Complex Systems, Emergence, Complexity and Computation 14, p. 143, Springer (2015). arXiv:1406.5847.
  - [54] J. Dowling and K. Seshadreesan, *Quantum Optical Technologies for Metrology, Sensing, and Imaging*, J. Light. Technol. **33**, 2359 (2015).
  - [55] K. Macieszczak, M. Guta, I. Lesanovsky and J. P. Garrahan, *Dynamical phase transitions as a resource for quantum enhanced metrology*, Phys. Rev. A **93**, 022103 (2016).
  - [56] K. Jacobs, *Quantum Measurement Theory and its Applications*, Cambridge University Press (2014).
  - [57] A. Lumino, E. Polino, A. S. Rab, G. Milani, N. Spagnolo, N. Wiebe and F. Sciarrino, *Experimental phase estimation enhanced by machine learning*, Phys. Rev. Applied **10**, 044033 (2018).